Low Complexity Rake Receivers in Ultra-Wideband Channels

Dajana Cassioli, *Member, IEEE*, Moe Z. Win, *Fellow, IEEE*, Francesco Vatalaro, *Senior Member, IEEE*, and Andreas F. Molisch, *Fellow, IEEE*

***Abstract*— One of the major issues for the design of ultra-wideband (UWB) receivers is the need to recover the signal energy dispersed over many multipath components, while keeping the receiver complexity low. To this aim we consider two schemes for reduced-complexity UWB Rake receivers, both of which combine a subset of the available resolved multipath components. The first method, called partial Rake (PRake), combines the *first* arriving multipath components. The second is known as selective Rake (SRake) and combines the *instantaneously strongest* multipath components. We evaluate and compare the link performance of these Rake receivers in different UWB channels, whose models are based on extensive propagation measurements. We quantify the effect of the channel characteristics on the receiver performance, analyzing in particular the influence of small-scale fading statistics. We find that for dense channels the performance of the simpler PRake receiver is almost as good as that of the SRake receiver, even for a small number of fingers. In sparse channels, however, the SRake outperforms the PRake significantly. We also show that for a fixed transmitted energy there is an optimum transmission bandwidth.**

***Index Terms*— Reduced complexity Rake receivers, partial Rake, selective Rake, UWB propagation channel, stochastic tapped-delay line model**

I. Introduction

ULTRA-WIDE BANDWIDTH (UWB) spread-spectrum (SS) techniques for multiple access wireless communications were first proposed in the 1990s to meet the demands of future wireless networks [1], [2]. The use of an extremely wide transmission bandwidth results in desirable capabilities including position location and ranging (from which communications services may benefit), immunity to narrowband interference, multiple access capability for broadband wireless communications, covert transmission, possible easier material penetration, and robustness against multipath fading [3]–[15].

Commercial interest in UWB techniques increased significantly after the US Federal Communications Commission (FCC) allowed *unlicensed* UWB communications [16] subject to certain constraints on the spectral properties of the emitted radiation. At the same time, the Task Group (TG) 3a was established within the IEEE 802.15 to define a standard for high data rate communication systems based on UWB technology. Later, the IEEE 802.15 TG 4a was formed to develop a standard for low data rate applications with high-precision ranging capability. Due to its high versatility, UWB technology was also included in this new standard. Two of the physical layer schemes that have been proposed for those standards are based on Impulse Radio [2], [3], [17]–[20], and direct-sequence (DS) [21] SS techniques.[1]

One of the key advantages of UWB signals is the immunity to fading. Depending on the bandwidth, a receiver can resolve multipath components (MPCs) whose path lengths differ by a few tens of centimeters, e.g., 15 cm for a signal bandwidth of 2 GHz. An increase in the transmission bandwidth improves the capability of resolving MPCs. Each of the resolved MPCs can be viewed as independently fading, thereby providing a high degree of diversity (delay diversity, frequency diversity) for the transmission [23]. However, in order to utilize the available diversity, the receiver must be able to extract and process the different MPCs.

A Rake receiver can exploit the high degree of diversity that results from a large number of MPCs. Combining *all* resolvable paths as in the *all-Rake (ARake)* receiver provides the optimal performance [24]–[27]. However, the number of MPCs that can be utilized in a typical Rake combiner is limited by power consumption constraints, complexity considerations, and the availability of channel estimates [28]. In typical UWB scenarios, the available number of MPCs at the receiver is often more than 100 [28]–[34]; hence the ARake UWB receiver serves only as a benchmark and provides a bound on the performance that is achievable by other suboptimal combining schemes. The complexity can be reduced, at the price of a performance penalty, by employing the *selective Rake (SRake)* receiver structure, which combines a subset of the available resolved MPCs, namely the instantaneously strongest L_b MPCs [24]–[27], [35]. The SRake provides a

Manuscript received May 26, 2004; revised July 30, 2005; accepted November 10, 2005. The associate editor coordinating the review of this paper and approving it for publication was R. Murch. This work was supported, in part, by the Charles Stark Draper Laboratory Reduced Complexity UWB Communication Techniques Program, the Office of Naval Research Young Investigator Award N00014-03-1-0489, the National Science Foundation under Grants ANI-0335256 and ECS-0636519, DoCoMo USA Labs, institutional cooperation grant form Swedish STINT, and an INGVAR grant of the Swedish Strategic research foundation. Part of this work has been presented at ICC 2002 and ICC 2003.

D. Cassioli is with the RadioLabs Consortium, Electric and Information Engineering Department, University of L'Aquila, 67040 Poggio di Roio, L'Aquila, Italy (e-mail: dajana.cassioli@radiolabs.it).

M. Z. Win is with the Laboratory for Information and Decision Systems (LIDS), Massachusetts Institute of Technology (MIT), Cambridge, MA, 02139, USA (e-mail: moewin@mit.edu).

F. Vatalaro is with the Electronic Engineering Department, University of Rome "Tor Vergata" viale Politecnico 1, 00133 Roma, Italy (e-mail: vatalaro@uniroma2.it).

A. F. Molisch was with AT&T Labs - Research. He is now with Mitsubishi Electric Research Labs, Cambridge, MA, 02139, USA, and also at the Department of Electroscience, Lund University, Lund, Sweden (e-mail: Andreas.Molisch@ieee.org).

Digital Object Identifier 10.1109/TWC.2007.04343.

[1]A third scheme, based on orthogonal frequency division multiplexing (OFDM) combined with time-frequency interleaving [22] does not involve the Rake receiver architecture that are the focal point of this paper, and will not be discussed here.

TABLE I
SUMMARY OF THE CHANNEL MODELS USED IN THE ANALYSIS.

	Frequency	Amplitudes	Comments
LF model	0.3-0.8 GHz	Nakagami (m varies with delay)	*Dense* channel: almost continuous rays' exponential decay
HF model	3.1-10.6 GHz	Lognormal	*Sparse* channel: some resolvable delays are empty (very high resolution)
Filtered HF model	3.1-3.6 GHz	Tend to Rayleigh	First path is not necessarily the strongest one; generally, PDP is sparse
Rayleigh-equivalent	0.3-0.8 GHz	Nakagami $m = 1$	Comparison with conventional wireless systems

reduction in the number of correlators and thus reduces power consumption. However, the selection procedure still requires full channel estimation, which may not be easily available.

In this paper we propose a simpler *partial Rake (PRake)* receiver structure, which combines the first arriving L_{p} paths out of the available resolved MPCs.[2] Thus this technique requires only synchronization, but not full channel estimation.[3] We compare the performance of PRake, SRake and ARake receivers that employ maximal-ratio combining [39]–[43] in *realistic* UWB channels.[4] We analyze the signal-to-noise ratio (SNR) statistics at the combiner output and the bit error probability (BEP) of these Rake receivers using several widely used channel models. We consider both the IEEE 802.15.3a channel model, suitable for simulating UWB systems that operate in the $3.1 - 10.6$ GHz range, and a channel model that is based on baseband pulse measurements [29]–[31]. We analyze the influence of small-scale fading statistics and the influence of a "sparse" channel model (such as the IEEE 802.15.3a) on the performance of different Rake structures. Finally, we investigate the dependence of both BEP and output SNR on the system bandwidth. We show that for a bandwidth of less than approximately 1 GHz, the performance improvement of the SRake as compared to the simpler PRake is quite small if the fading is Nakagami (a typical case for UWB), whereas larger improvements result in Rayleigh fading channels. For much larger bandwidths (up to 7.5 GHz), the PRake is not a good choice regardless of the fading statistics.

The rest of the paper is organized as follows. In Section II we present the channel models employed in the analysis. Sections III and IV.A discuss the SNR distributions and BEPs, respectively, for SRake, PRake, and ARake structures. The impact of the bandwidth on the BEP is investigated in Section IV.B. A summary and conclusions are presented in Section V.

II. CHANNEL MODELS

We consider several UWB channel models to evaluate the receiver performance. A low-frequency (LF) model, proposed in [31] is based on experimental data collected in an office environment using baseband 1 ns pulses. The antennas further modified the pulse spectrum, especially at the lowest frequencies towards zero, resulting in a 3-dB bandwidth of about 500 MHz, from 300-800 MHz. A high-frequency (HF) model, designed for 3.1-10.6 GHz, has recently been developed by the IEEE 802.15.3a for the simulation of FCC-compliant communication systems [32], [44].

The most important differences between this HF model and the LF model lie in the arrival statistics of the MPCs and in the distributions of MPCs' amplitudes. The HF model is *sparse*, i.e., there are resolvable delay bins that do not carry significant power mainly due to the use of much larger transmission bandwidths. Concerning the amplitudes' distributions, the HF model is lognormal while the LF model is Nakagami. The variance of the lognormal distribution of the HF model is assumed to be independent of delay, whereas the m-parameters of the Nakagami distributions of the LF model decrease with delay.

We consider the HF model in the whole bandwidth of 7.5 GHz as well as in a bandwidth of 500 MHz, obtained by filtering the realizations of the HF channel impulse response over the band 3.1–3.6 GHz (referred to as the "filtered HF channel" in the following). We consider this frequency range because it allows an effective comparison with the LF model, using the same bandwidth but exhibiting different amplitude statistics. Indeed, several lognormal-fading MPCs interfering at each resolvable delay lead to a path amplitude with quasi-Rayleigh distribution. The power delay profile (PDP) of the HF model is generally not monotonic, but rather sparse, and the direct path (i.e., the first MPC of the PDP) is not necessarily the strongest one.

Finally, we also evaluate the receiver performance in a Rayleigh-equivalent UWB channel in the same band as the LF model.[5] This is of interest because previous performance analysis of UWB systems has often assumed Rayleigh fading, owing to the lack of a suitable channel model.

Table I summarizes the channel models used in the following analysis and their main characteristics. Some details about the LF and HF models are provided in the following.

A. Low-Frequency Channel Model

The LF channel model [31] has been accepted by the channel model subcommittee of the IEEE 802.15.4a standardization group for performance evaluation of UWB systems operating below 1 GHz [45].

The LF model is based on a measurement campaign performed in a typical office building [29], [30]. It characterizes the shape of the PDP using a tapped-delay line model where the k-th tap is determined by the path gain G_k and the delay $\tau_k = (k-1)\Delta\tau$, where $\Delta\tau = 2$ ns is the resolution of the considered system.[6] The model distinguishes between large- and small- scale fading, hence the *local path gains* G_k are derived by the superposition of these two effects. The model parameters are summarized in Table II, where the global

[2]A number of papers have taken up this concept after we first proposed it in our conference paper [36].

[3]Synchronization techniques for UWB signals can be found in [37, 38].

[4]Maximal-ratio combining is optimum for noise-limited systems with ideal autocorrelation properties of the spreading sequence, as well as ideal channel estimation. In the following, we will assume that these conditions are fulfilled.

[5]The Rayleigh-equivalent channel model is obtained from the LF model assuming the m-parameter equal to 1 for all delay bins.

[6]By definition, the delay bin of the first quasi line-of-sight (LOS) path begins at $\tau_1 = 0$. The model prescribes the statistics of the path gains and their dependence on the delays τ_k.

TABLE II
STATISTICAL MODELS AND PARAMETERS FOR THE LF MODEL.

GLOBAL PARAMETERS $\Rightarrow \overline{G}_{\rm tot}$ and $\overline{G}_k$	
Path Loss	$PL = \begin{cases} 20.4 \cdot \log_{10}\left(\frac{d}{d_0}\right) & d \le 11\text{m} \\ -56 + 74 \cdot \log_{10}\left(\frac{d}{d_0}\right) & d > 11\text{m} \end{cases}$
Shadowing	$\overline{G}_{\rm tot} \sim \mathcal{L}_N\,(-PL,\ 4.3)$
Decay Constant Power Ratio	$\varepsilon \sim \mathcal{L}_N\,(16.1,\ 1.27)$ $r \sim \mathcal{L}_N\,(-4.0,\ 3.0)$
LOCAL PARAMETERS $\Rightarrow G_k$	
Energy Gains	$G_k \sim \mathcal{G}\,(\overline{G}_k,\ m_k)$
m values	$m_k \sim \mathcal{T}_N\,(\mu_{\rm m}(\tau_k),\ \sigma^2_{\rm m}(\tau_k))$ $\mu_{\rm m}(\tau_k) = 3.5 - \frac{\tau_k}{73}$ $\sigma^2_{\rm m}(\tau_k) = 1.84 - \frac{\tau_k}{160}$

TABLE III
PARAMETERS FOR THE IEEE 802.15.3A MODEL

Parameters	CM1	CM2	CM3	CM4
Λ [1/nsec]	0.0233	0.4	0.0667	0.0667
λ [1/nsec]	2.5	0.5	2.1	2.1
Γ	7.1	5.5	14.00	24.00
γ	4.3	6.7	7.9	12
σ_1 [dB]	3.3941	3.3941	3.3941	3.3941
σ_2 [dB]	3.3941	3.3941	3.3941	3.3941
σ_x [dB]	3	3	3	3

parameters characterize the large-scale fading and the local parameters characterize the small-scale statistics.[7]

The small-scale averaged PDP (SSA-PDP) is completely specified according to:

$$\overline{G}(\tau) = \frac{\overline{G}_{\rm tot}}{1 + rF(\varepsilon)} \left\{ \delta(\tau - \tau_1) + \sum_{k=2}^{L_r} \left[r e^{-\frac{(\tau_k - \tau_2)}{\varepsilon}} \right] \delta(\tau - \tau_k) \right\}, \tag{1}$$

where $\overline{G}_{\rm tot}$ is the total mean energy, given by the mean path-loss (described by a dual-slope model) and the shadowing (modeled as lognormal fading). The time decay constant, ε (measured in ns), is also modeled as a random variable, as is the power ratio $r = \overline{G}_2/\overline{G}_1$, which indicates the amount of "extra" power (compared to the pure exponential decay law) carried in the first bin. Finally, $F(\varepsilon) = 1/(1 - \exp(-\Delta\tau/\varepsilon))$ is a normalization constant [31].

Over the small-scale region, the G_k are random variables around the mean values $\overline{G}_k$ given by the SSA-PDP in (1) at each delay bin τ_k. Their probability density function (pdf) can be approximated by a Gamma distribution (i.e., the amplitude distribution is Nakagami) with mean $\overline{G}_k$ and *shape* parameter m_k. The parameters m_k are Gaussian-distributed random variables whose mean and variance decrease with excess delay.[8] Implementation details can be found in [31].

[7]In Table II, $\mathcal{L}_N(x, y)$ denotes a *lognormal* distribution with mean x and variance y of the underlying Gaussian distribution; $\mathcal{G}(x, y)$ denotes a *gamma* distribution with mean x and shape parameter y; finally, $\mathcal{T}_N(x, y)$ denotes a *truncated Gaussian* distribution with mean x and variance y.

B. High-Frequency Channel Model

The HF channel model has been established by the IEEE 802.15.3a standardization group for evaluating various proposals for high-data-rate UWB communications systems [32], [44]. This model is intended to represent the channel characteristics in the frequency range from 3.1 to 10.6 GHz. It is based on the Saleh-Valenzuela model [46], which represents a "clustering" of the paths. The channel impulse response is defined as

$$h_i(t) = X_i \sum_{l=0}^{L} \sum_{k=0}^{K} a^i_{k,l}\, \delta(t - T^i_l - \tau^i_{k,l}) \tag{2}$$

where $a^i_{k,l}$ is the tap weight associated with the k-th ray of the l-th cluster, X_i represents the log-normal shadowing, and i refers to the i-th realization; K is the number of rays in each cluster, and L is the number of clusters. The distributions of cluster and ray arrival times, respectively, are given by

$$p(T_l|T_{l-1}) = \Lambda \exp[-\Lambda(T_l - T_{l-1})], \qquad l > 0$$
$$p(\tau_{k,l}|\tau_{(k-1),l}) = \lambda \exp[-\lambda(\tau_{k,l} - \tau_{(k-1),l})], \quad k > 0.$$

The channel coefficients are defined as $a_{k,l} = p_{k,l}\ \xi_l\ \beta_{k,l}$, where $p_{k,l} \in \{+1, -1\}$ is equiprobable and represents the signal inversion due to reflections. The parameter ξ_l reflects the fading associated with the l-th cluster, and $\beta_{k,l}$ corresponds to the fading associated with the k-th ray of the l-th cluster. The distribution of the channel coefficients is given by $|\xi_l \beta_{k,l}| = 10^{(\mu_{k,l} + n_1 + n_2)/20}$, where $n_1 \sim \mathcal{N}(0, \sigma_1^2)$ and $n_2 \sim \mathcal{N}(0, \sigma_2^2)$ are independent Gaussian variables corresponding to the fading of each cluster and ray, respectively. The parameters $\mu_{k,l}$ are given by

$$\mu_{k,l} = \frac{10\ln(\Omega_0) - 10\ T_l/\Gamma - 10\ \tau_{k,l}/\gamma}{\ln(10)} - \frac{(\sigma_1^2 + \sigma_2^2)\ln(10)}{20}, \tag{3}$$

where Ω_0 is the mean energy of the first path in the first cluster, T_l and $\tau_{k,l}$ are the excess delays of cluster l and of the k-th ray in cluster l, respectively. Γ is the clusters' decay constant and γ is the rays' decay constant. Finally, the total energy contained in the terms $\{a^i_{k,l}\}$ is normalized to unity for each realization, because the lognormal shadowing of the total multipath energy is characterized by X_i, for which $20\log_{10} X_i \sim \mathcal{N}(0, \sigma_x^2)$. Table III summarizes the parameters of the model for the four different environments defined by the IEEE 802.15.3a standard.

Based on the work of [47], IEEE 802.15 also recommends a new way of modeling the path-loss. While there is still shadowing superimposed on a polynomial power decay law with the logarithm of distance, the decay exponent n and the shadowing variance σ have now become random variables. Table IV shows the path-loss at a distance of 1 m, L_0, as well as mean and standard deviation for LOS and non-LOS (NLOS) situations. The distributions of all variables are modeled as Gaussian.

[8]Note that the Gaussian distribution is truncated, so that the (non-physical) values $m < 0.5$ cannot occur.

TABLE IV
STATISTICAL VALUES OF THE PATH-LOSS MODEL PARAMETERS [47]

	LOS		NLOS	
	Mean	**Std. Dev.**	**Mean**	**Std. Dev.**
L_0 **(dB)**	47	NA	50.5	NA
n	1.7	0.3	3.5	0.97
σ **(dB)**	1.6	0.5	2.7	0.98

III. THE DISTRIBUTION OF THE SNR

The Rake combiner "rakes up" (appropriately sums up) the signals from the different Rake fingers to produce a decision variable, which is then processed by a data detector. The detector "sees" only an equivalent channel created by the cascade of the physical radio channel and the Rake combiner. Thus, the quantity that determines the receiver performance is the SNR at the Rake output. More specifically, the system performance is determined by the pdf of either the instantaneous SNR or the small-scale-averaged SNR, depending on the receiver characteristics. The former is the relevant quantity for all systems that have a "memory" much shorter than the channel coherence time. The "memory" of the system in this context could be caused, for example, by coding, interleaving, perception of the human ear, or the size of typical data structures (files) to be transmitted. If the length of the system "memory" is comparable to, or larger than, the coherence time of the channel, the relevant quantity is the pdf of the small-scale-averaged SNR.

We obtain the pdfs of the SNR as follows. We generate a local PDP according to each of the models described in Sec. II, and we select either all available L_{r}, the strongest L_{b}, or the first L_{p} taps for the ARake, the SRake, or the PRake, respectively. We then add the SNRs of the selected taps, yielding the SNR at the Rake combiner output. This procedure is then repeated for several different channel realizations. The histograms of such channel ensembles give a discrete approximation of the pdf of the SNR. Similarly, the pdf of the small-scale averaged SNR is obtained by considering the SSA-PDP. In the following subsections, we will discuss these distributions in the considered channels.

A. SNR Distributions in the LF Channels

Figure 1 (a) shows the cumulative distribution functions (CDFs) of the SNR for the LF model, for both SRake and PRake. It can be seen that the SRake receiver has a slightly better energy capture performance than the PRake, especially for a small number of fingers. For example, SRake can capture approximately 2 dB more energy than PRake for the case of 2 fingers. The difference shrinks to less than 0.5 dB when the number of fingers increases to 16.

This behavior can be attributed to the fact that the average PDP is exponentially decaying and that the fading severity parameter m of the Nakagami distribution is greater than 1 for the amplitudes of the first several arriving bins. Indeed, as outlined in Sec. II-A, the m-parameters (modelled as random variables) vary with the excess delay, i.e., a different m-parameter belongs to each delay bin. In particular, since the mean of the m-parameters follows a linear decay with excess

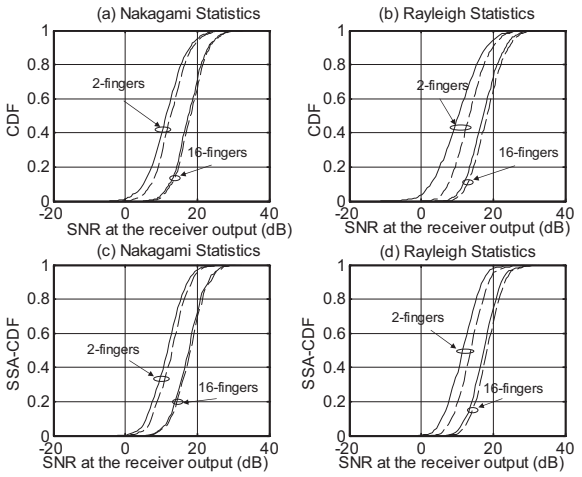

Fig. 1. The CDFs and the small-scale averaged CDFs (SSA-CDFs) of the SNR at the output of the PRake (solid) and SRake (dashed) receivers combining 2 and 16 fingers in the LF model assuming Nakagami and Rayleigh fading. The average transmitted SNR is set to 20 dB and the transmitter-receiver (Tx-Rx) distance to 1 m.

delay (see Table II), in general the m-parameters of the smaller excess delays are greater than 1, while $m = 1$ is observed at large excess delays. If the channel taps were not fading, then the PRake and the SRake would perform identically: as the PDP is monotonically decaying, the PRake and the SRake would pick the same fingers. In the presence of fading, however, there is a finite probability that one of the first taps is in a deep fade (even though on average they carry the largest energy). Such taps can be avoided by the SRake, but not by the PRake (by definition). The probability for such situations, however, is relatively small for the considered channel model: Nakagami fading leads to smaller variations of the instantaneous amplitudes than, e.g., Rayleigh fading (see also below). Especially for the paths with small excess delays, the m-parameter is considerably larger than unity, implying that the instantaneously strongest paths are still concentrated in the first portion of the excess delay axis.

Figure 1(b) shows the performance of SRake and PRake in a channel with Rayleigh amplitude statistics. It can be seen that the performance of a PRake receiver is considerably worse than that of an SRake in such a channel, and the slopes of the CDFs are quite different. The reason for this is that for Rayleigh-fading taps, there is a larger probability that one of the first taps is in a deep fade. For Nakagami fading,[9] on the other hand, the fading depth is much smaller, so a tap that carries large average energy also has a high probability of carrying high instantaneous energy. Conversely, from the comparison of Fig. 1(a) with Fig. 1(b), it emerges that with an SRake, a Rayleigh-fading channel actually gives a *higher* average energy than a Nakagami-fading channel. This can be explained by the fact that Rayleigh fading leads to a larger probability not only of deep fading dips, but also of higher amplitudes than Nakagami fading. Those higher amplitudes are exploited by the SRake. The PRake, on the other hand, cannot exploit those higher amplitudes and always performs worse in Rayleigh fading due to a larger probability of deep

[9]To simplify notation, henceforth we use "Nakagami fading" to denote "Nakagami fading with $m > 1$".

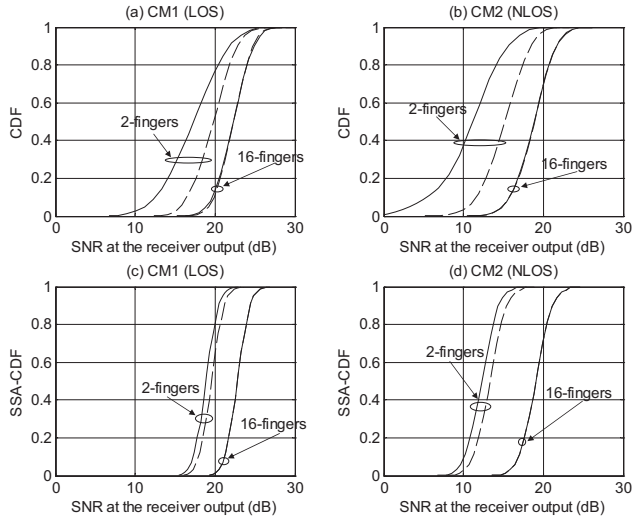

Fig. 2. The CDFs and the SSA-CDFs of the SNR at the output of the PRake (solid) and SRake (dashed) receivers combining 2 and 16 fingers in the filtered HF model with a bandwidth of 0.5 GHz (3.1 − 3.6 GHz). The average transmitted SNR is set to 60 dB and the Tx-Rx distance to 1 m.

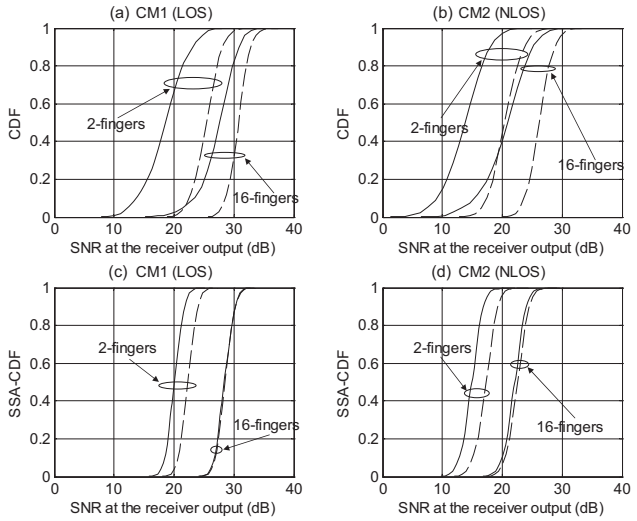

Fig. 3. The CDFs and the SSA-CDFs of the SNR at the output of the PRake (solid) and SRake (dashed) receivers combining 2 and 16 fingers in the HF model with a bandwidth of 7.5 GHz (3.1 − 10.6 GHz). The average transmitted SNR is set to 60 dB and the Tx-Rx distance to 1 m.

fading dips compared to Nakagami fading.

If the receiver (or transmitter) moves, then the channel changes within a finite time, and the system memory can thus extend over many small-scale realizations of the channel. In this case a system would average the SNR over the small-scale fading. Note that we have assumed here that the number and delays of the Rake fingers stay fixed during the movement (this approach might be used, e.g., in order to avoid frequent re-estimation of the complete channel); the results would have been different if the SRake is adjusted to the instantaneously-best fingers and averaged over the resulting SNR.[10]

Figures 1(c) and 1(d) plot the CDF of the small-scale-averaged SNR for different numbers of fingers. We note that the averaging leads to a steeper CDF (compared to the distribution of the local SNR), especially for a PRake in Rayleigh fading with a small number of fingers. For a large number of fingers, the difference in the CDFs (between the local SNR and the SSA-SNR distributions) is small, since the local SNR CDFs are already steep due to the high degree of diversity. Similar behaviors can also be observed for Nakagami fading.

B. SNR Distributions in the HF Channels

Figure 2 shows the CDFs of the SNR for the filtered HF model in LOS and NLOS conditions.[11] A system bandwidth of 500 MHz in the frequency range from 3.1 to 3.6 GHz is considered. It can be seen in Fig. 2 (a) that, for a 2-finger Rake, the performance difference between the SRake and the PRake in the LOS channel CM1 is larger than that in the LF model. The reason for this lies in the different fading statistics: as mentioned in Sec. II, the fading is more Rayleigh for the filtered HF model than for the LF model. The difference in mean SNR between SRake and PRake is about 3 dB, but for the 10% outage probability, the SNR difference increases to about 5 dB. This necessarily implies that the first path is not always the strongest, otherwise, if the first path were the strongest, the difference between SRake and PRake would be at most 3 dB. This difference is due to the SRake capability of tracking the instantaneously best second path, while, in the worst case, the second finger of the PRake may even capture zero energy. In the NLOS case, shown in Fig. 2 (b), the performance of the PRake is worse, because in that scenario the first component can be weak and can even be followed by less energy in the subsequent delay bin. On the other hand, we find that for a 16-finger of PRake, there is no discernible difference between SRake and PRake. This is due to the fact that 16 fingers of PRake cover 32 ns delay, covering almost the entire support of the impulse response.

Figure 3 considers the HF model with the full bandwidth (7.5 GHz). It can be seen in Fig. 3 (a) that in the LOS channel CM1 the performance difference between SRake and PRake is considerably larger than those for the LF model and the filtered HF model. This difference is attributable to the "sparseness" of the channel model. With high probability, the tap immediately after the LOS component does not carry energy and thus the 2-finger PRake does not provide any diversity gain. The SRake, on the other hand, gathers energy from the second finger and thus provides a diversity gain. It is also interesting to note that the *average* gain of the SRake compared to the PRake is larger than 3 dB. This can be explained by the fact that the LOS component is not always the instantaneously strongest one. This fact can be verified by a visual inspection of the channel realizations specified in the IEEE 802.15.3a model. In the NLOS channel model CM2, shown in Fig. 3 (b), the performance of the PRake is much worse. In that scenario, the first component can be very weak, and even less energy can follow in the subsequent delay bin. For the 16-finger case, the difference between the two Rake structures is smaller, but still has several dB of difference. The reason is that even the 16 fingers of a PRake cover only a small portion of the support of the impulse response, namely $16 * 0.133$ ns $= 2.128$ ns.

[10]Note that the latter case would require more frequent estimation of the full channel impulse response.

[11]With reference to Table III, these correspond to the sets of parameters in the CM1 and CM2 columns, respectively.

This is in contrast to the filtered case, where the 16 fingers of the PRake cover 32 ns.

When considering the small-scale averaged case, we find that the difference in performance between the two Rake structures is reduced for both the filtered HF channel and the full-bandwidth HF channel (similar to the LF model). However, the full-bandwidth case exhibits the largest difference. For the LOS case, shown in Fig. 3(c), the PRake shows slightly less than 3 dB performance loss (compared to the SRake). This is consistent with the fact that *on average*, the LOS tap is the strongest, followed by a no-energy-carrying tap; furthermore other existing taps carry almost as much energy as the LOS tap. The slope of the CDF is determined by the shadowing. Similar statements are true for the NLOS case, as shown in Fig. 3 (d); however, the performance loss of the PRake is larger, as the first tap is not necessarily the strongest, even on average. Note that this is a basic difference between the LF and the HF channel models. Signals with low frequency components can penetrate objects quite well or can easily diffract around them. For this reason, the first-arriving MPCs are always strong. At microwave frequencies (HF model), however, indirect propagation paths that involve one or more reflections can carry large energy, so that the average PDP shows a non-monotonic behavior. This in turn leads to the difference in the PRake performance shown in Fig. 3(d) and 1(c).

IV. The Bit Error Probability

In this section, we evaluate the uncoded BEP of the SRake and PRake structures in different channels. We assume that the fading is sufficiently slow compared to the symbol duration (i.e., the inverse of the channel Doppler frequency is smaller than the symbol duration). In that case, the BEP is obtained by averaging the conditional BEP, $P_{\mathrm{e}|\gamma_{\mathrm{b}}}$, conditioned on the received instantaneous (local) SNR per bit, γ_{b}, at the Rake output, over the pdf $p_{\gamma_{\mathrm{b}}}(\cdot)$ as given in [23], [43]:

$$P_{\mathrm{e}} = \int_0^{\infty} P_{\mathrm{e}|\gamma_{\mathrm{b}}}(x) p_{\gamma_{\mathrm{b}}}(x) dx \,. \tag{4}$$

We consider binary pulse position modulation (PPM) with coherent detection. Thus, the conditional BEP is given by [43]:

$$P_{\mathrm{e}|\gamma_{\mathrm{b}}} = Q\left(\sqrt{\gamma_{\mathrm{b}}}\right) \tag{5}$$

where $Q(x) = \frac{1}{\sqrt{2\pi}} \int_x^{\infty} e^{-t^2/2} dt, \quad x \geq 0$ or equivalently $Q(x) = \frac{1}{2}\mathrm{erfc}\left(\frac{x}{\sqrt{2}}\right)$.

A semi-analytical calculation of the BEP can be obtained by averaging $P_{\mathrm{e}|\gamma_{\mathrm{b}}}$ over the channel ensemble, namely one thousand realizations of the channel impulse response for each value of the average SNR.

Following the same procedure outlined in Sec. III to obtain the distributions of the SNR for various Rake receivers, we generate a channel ensemble for each of the considered UWB channel models. However, unlike in the previous section, we consider here a normalized channel with unit total energy. In other words, the shadowing is eliminated by appropriate normalization. This allows a better insight into the different Rake receiver structures since the relative comparison between them is not influenced by the total received energy.

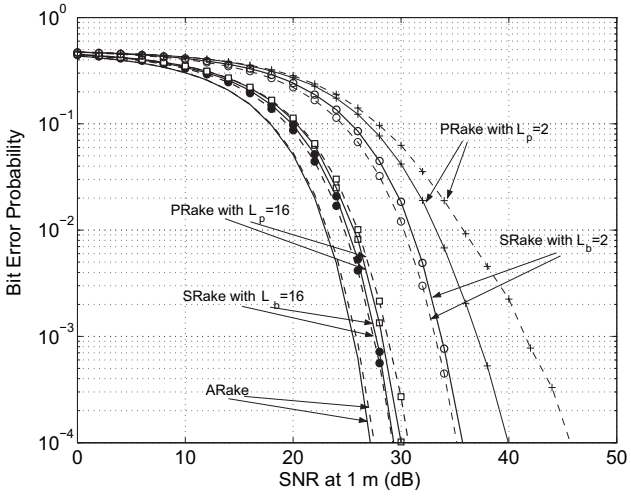

Fig. 4. A comparison of the effects of the amplitude distribution when the small scale statistics are modelled by a Nakagami (solid) or a Rayleigh distribution (dashed), while the average PDP profile follows an exponential decay in both cases. 2 and 16 fingers SRake and PRake are considered. The Tx-Rx distance is 6 m. As a benchmark the ARake performance is also plotted.

We will compare both the gain in SNR (to achieve a target BEP, e.g., 10^{-3}), and the diversity order (i.e., slope of the BEP curves at very high SNRs). Unless otherwise specified, the BEP curves presented in the following sections are plotted against the average SNR per bit at the reference distance $d_0 = 1$ m.

A. BEP in LF and HF Channels

Figure 4 shows the BEP as a function of normalized SNR at the Rake output for the ARake, the SRake, and the PRake in the LF channel. We first discuss the results for the case of SRake and PRake with two fingers. As anticipated, the ARake has the best performance, having an SNR advantage of almost 10 dB (for both the Nakagami and Rayleigh fading) as compared to the SRake at a BEP=10^{-3}. The PRake performs somewhat worse than the SRake, leading to a loss in SNR of about 4 dB (for Nakagami fading) and 9 dB (for Rayleigh fading) at BEP=10^{-3}. Moreover, the PRake and SRake curves have different slopes, for example, the performance difference between the two receivers is small at BEP=10^{-1}. These results again demonstrate the importance of using the correct UWB fading distribution. Otherwise, wrong conclusions about the relative performance of different receiver architectures could be drawn.

Figure 4 also depicts the performance when the number of Rake fingers is increased to 16. Naturally, the performance loss of the SRake compared to the ARake decreases; it becomes approximately 2 dB (for both Nakagami and Rayleigh fading) at BEP= 10^{-3}. We also note that the PRake and the SRake have approximately the same diversity order and differ by only about 1 dB. The reasons for this similar performance have been discussed in Sec. III.

Figure 5 shows the BEP for the four scenarios of the HF channel model listed in Table III, with the full 7.5 GHz bandwidth. The differences between the 2-finger Rakes and the ARake in the HF channel are much larger than those in the LF channel: 10 dB (for CM1) and 15 dB (for CM4) for the

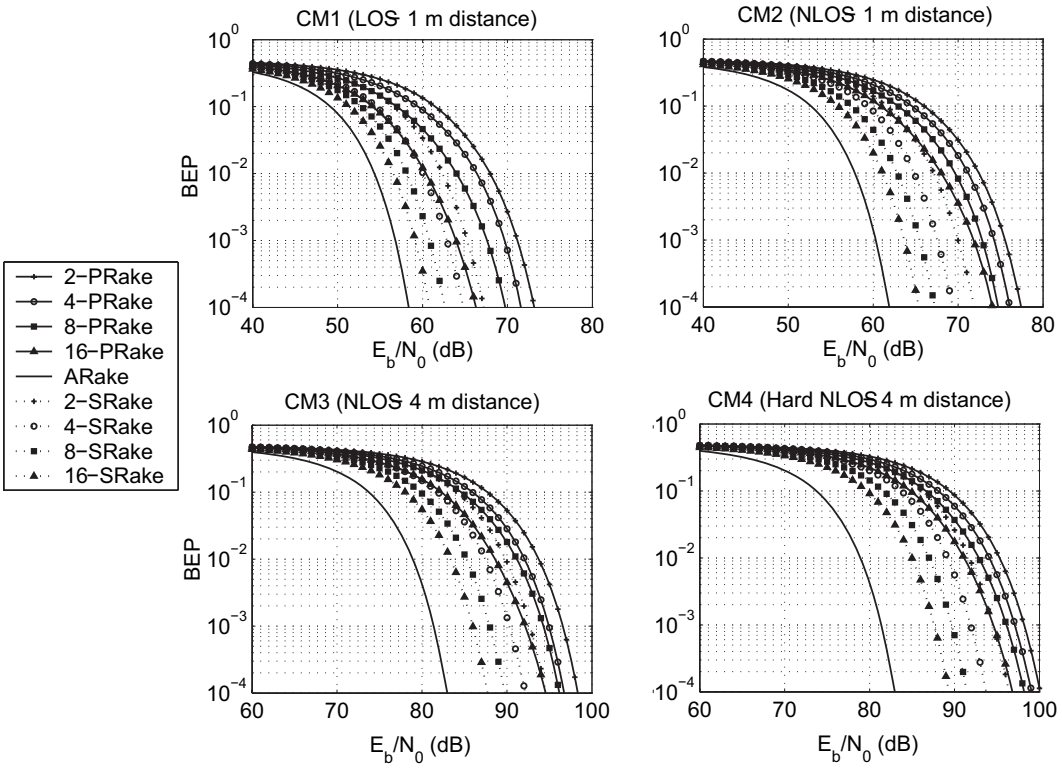

Fig. 5. The BEP vs. $E_{\rm b}/N_0$ for PRake and SRake in the HF channel model with the full transmission bandwidth (7.5 GHz). The path-loss model of [47] is assumed, while the shadowing is normalized.

SRake, as well as 15 dB (for CM1) and 18 dB (for CM4) for the PRake at BEP=10^{-3}. The reason for this is that the energy is spread over more resolvable delay taps due to the larger transmission bandwidth. We also note that the performance difference between the SRake and the PRake in the HF channel is larger than that in the LF channel, the reasons for which have already been discussed in Sec. III.

B. BEP vs. Spreading Bandwidth

We now investigate the influence of the spreading bandwidth on the system performance.[12] The first effect we can expect from an increase of the spreading bandwidth is an increase of diversity gain, resulting in a performance improvement. This is obvious for the ARake, as the number of diversity paths is directly proportional to the spreading bandwidth. Nevertheless, the diversity gain also increases with spreading bandwidth for the SRake and the PRake, though the reasons in those cases are subtly different.

For the SRake, the number of combined diversity paths $L_{\rm b}$ remains fixed. However, in a dense multipath channel, the number of resolvable multipaths increases with the spreading bandwidth. This implies that the number of the available diversity paths, $L_{\rm r}$, out of which the SRake chooses to combine the diversity paths increases. Hence, the probability that all of the combined paths simultaneously fade decreases, and consequently, the BEP performance improves. This fact has been proven for Rayleigh fading channels [49].

For the PRake, the diversity gain is related to the PDP. In general, the diversity gain is highest for a uniform PDP [50, 51], while only a few fingers carry significant energy for a strongly decreasing PDP. The energy distribution among the resolved multipaths varies with the spreading bandwidth. In the extreme case of a narrowband system, only a single finger captures energy. For a very wide bandwidth system, each of the resolvable delay bin is very short (compared to the delay spread). Thus all fingers in PRake are placed within a small fraction of the PDP, each capturing (on average) almost the same amount of energy. This leads to the highest effective diversity gain. Since higher diversity gain means lower probability of fading dips, the BEP performance improves.

However, as the spreading bandwidth increases, the signal energy is dispersed among more resolvable multipaths, hence the amount of energy captured by a Rake receiver with a fixed number of fingers decreases. In other words, the loss in captured energy increases, essentially unlimited, as we increase the spreading bandwidth.[13] On the other hand, the BEP improvement due to diversity gain saturates as the spreading bandwidth increases.

Depending on the strength of these two counteracting effects due to an increase of spreading bandwidth (namely, the increase of the diversity gain and the decrease of the captured energy), we can anticipate a BEP-vs.-bandwidth curve to exhibit either a minimum or a monotonic behavior.

The existence of a minimum also depends on whether the system is *power* limited, or whether it is *power spectral density* (PSD) limited, for example, by FCC regulations. In the following, we will analyze the LF model under the assumption

[12]Theoretical analyses of the effect of spreading bandwidth have been given for Rayleigh-fading in [24]–[26], [48].

[13]Note that this argument is valid for a fixed transmit power. For a fixed transmit power spectral density, the energy captured by a fixed number of fingers stays approximately constant.

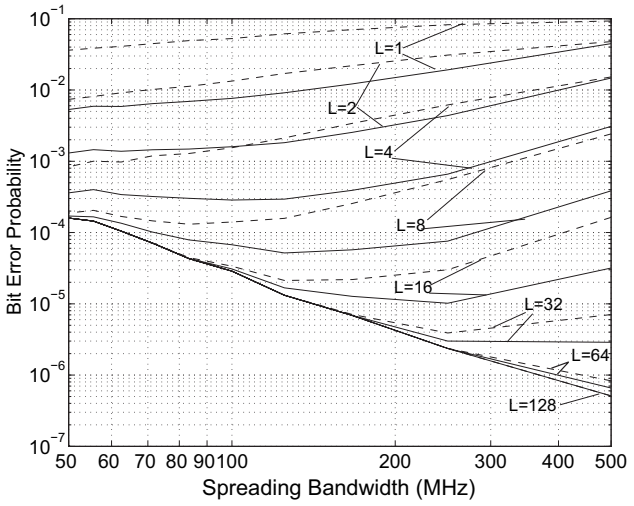

Fig. 6. The BEP vs. the spreading bandwidth in a Log-Log scale for different numbers of PRake (dashed) and SRake (solid) fingers in the Nakagami LF model. The Tx-Rx distance is 6 m and the average transmitted SNR is 30 dB.

of power limitation, and the HF model under the assumption of PSD limitation.

1) LF channel: Figure 6 plots the BEP in the LF channel as a function of the spreading bandwidth for different numbers of Rake fingers. It can be seen that there is indeed an optimum value which increases with the number of Rake fingers (for very high number of Rake fingers, the optimum is no longer visible on the plot). This is intuitively clear, as more fingers are capable of capturing the energy provided by a larger number of resolved paths.

At low spreading bandwidths some of the BEP curves merge. This occurs since only a few MPCs of the channel are resolved at low spreading bandwidth, and having more fingers does not provide an additional advantage. For example, suppose that only 10 paths carry energy, in which case it does not matter whether 16, 32, or more fingers are available; only 10 can be used, and the weight of the others is set to zero.

It is clear in Fig. 6 that the SRake outperforms the PRake. The difference in their performance decreases as the number of fingers increases. For the SRake the optimum bandwidth is at higher values - with the selective combining, more energy is collected.

2) HF channel: Figure 7 shows the results for the HF model with a constant PSD. Note that the BEP consistently improves as we increase the bandwidth. The reason for this effect is that, in order to keep the PSD constant while the energy is distributed among more taps, the energy per tap stays approximately constant leading to an improvement in the SNR at the Rake output and, consequently, in the BEP.[14] This energy increase is fully exploited by the SRake, which is able to track the instantaneously best paths and is thus immune to the sparseness of the channel. As shown in Fig. 7, the BEP for the SRake consistently decreases with the spreading bandwidth. On the other hand, the PRake is quite sensitive to the channel sparseness, as proven by the existence of a distinct minimum in the BEP curves: the larger the bandwidth, the larger the percentage of PRake fingers that collect no energy at all. Naturally, the minimum occurs at larger bandwidths for larger numbers of Rake fingers.

For a power limited system, the optimum bandwidth of a SRake receiver is always higher than that of a PRake in both the LF and the HF model. This can be explained by the fact that the average energy capture is higher for the SRake, so that more spreading can be used before the energy loss becomes prohibitive.

[14]The energy per tap stays approximately constant as long as the resolvable delay bin width is larger than the interarrival times of the multipath components.

V. Conclusions

We have analyzed the performance of low complexity Rake receivers in UWB indoor channels. In particular, we have introduced a PRake architecture, which exploits only the first arriving propagation paths. PRake receivers are usually less complex than conventional Rake receivers, since they do not require a complete channel estimation or a full adaptability. We have compared the performance of the PRake with that of the more complex SRake in different channels. Due to the different behaviors of propagation media at different frequencies, the comparison based on channel models valid for frequencies either below 1 GHz or above 3.1 GHz has allowed us to highlight which particular Rake architecture is most suitable for a given frequency range.

The characteristics of the LF channel, namely the exponentially decaying PDPs and the Nakagami fading, make a PRake performance almost as good as a SRake performance. In particular, our results show that, for a transmission bandwidth on the order of 1 GHz and a number of fingers greater than eight, the performance of the PRake receiver is similar to that of the SRake. This behavior is even more evident if the path gains have a Nakagami distribution with fading severity parameters m greater than 1, which is typical for UWB channels.

Conversely, the SRake outperforms the PRake for a large transmission bandwidth. In this case the path arrival times, rather than the path gain statistics, play a key role. The HF channel impulse response is sparse and some paths do not carry signal energy, an effect that is even more pronounced in NLOS situations, where the first arriving component is not necessarily the strongest one. In these channels, when accurate channel estimates are available, the full adaptability of the SRake allows for a better performance. We found that the relative difference between PRake and SRake strongly depends on the transmission bandwidth and the operating environment. In the HF channel, a system with a bandwidth of 7.5 GHz based on PRake loses more than 10 dB at a target BEP of 10^{-3} with respect to a similar system based on SRake reception. A PRake thus is a viable option only when the transmission bandwidth is considerably less than 7.5 GHz, i.e., the upper limit for the bandwidth prescribed by the current FCC regulations.

Finally, we have analyzed the Rake performance for different spreading bandwidths. We found that the optimum spreading bandwidth depends on (i) whether we use PRake or SRake, and (ii) whether we employ a constant transmit PSD or a constant transmit power.

Our results provide important guidelines for the design of

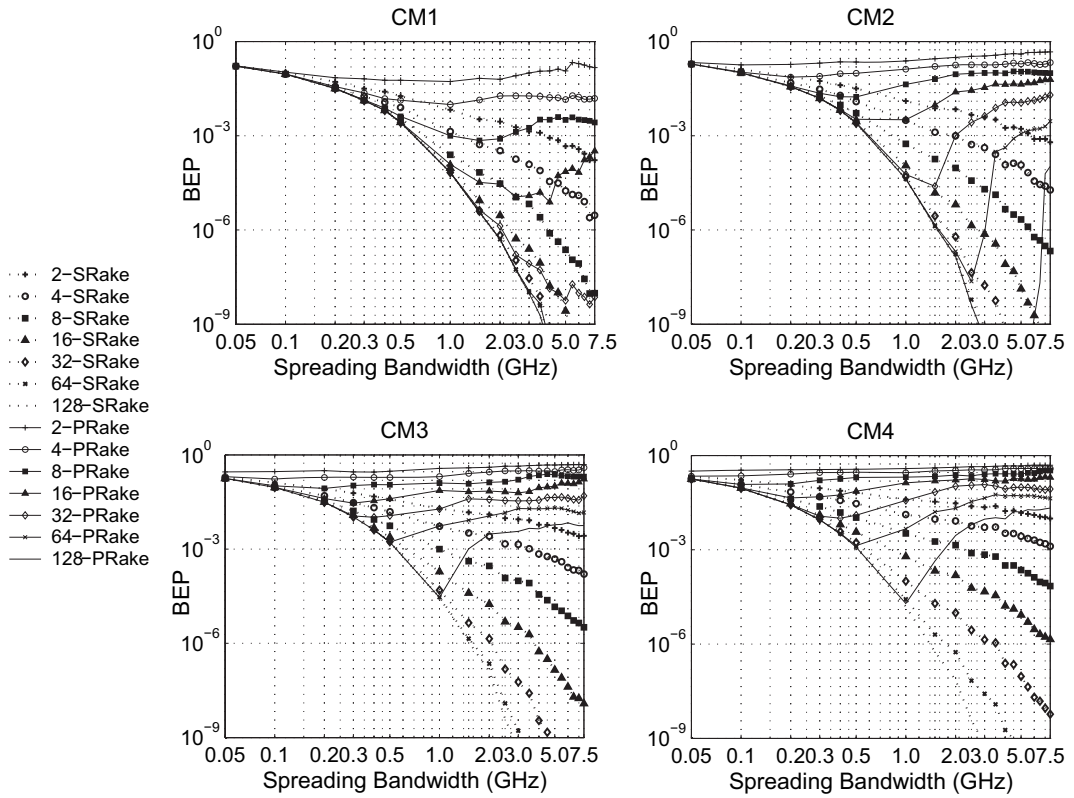

Fig. 7. The BEP vs. the spreading bandwidth (BW) in a Log-Log scale for PRake and SRake in the HF models filtered over the bands (3.1-3.1+BW) GHz. A constant PSD is assumed.

low complexity Rake receivers for both consumer and military applications.

ACKNOWLEDGEMENT

The authors would like to thank T. Q. S. Quek and I. Keliher for helpful discussions and careful reading of the manuscript.

REFERENCES

[1] R. A. Scholtz, "Multiple access with time-hopping impulse modulation," in *Proc. Military Comm. Conf.*, Oct. 1993, Boston, MA. Invited Paper.

[2] M. Z. Win and R. A. Scholtz, "Impulse radio: How it works," *IEEE Commun. Lett.*, vol. 2, pp. 36–38, Feb. 1998.

[3] M. Z. Win and R. A. Scholtz, "Ultra -wide bandwidth time-hopping spread-spectrum impulse radio for wireless multiple -access communications," *IEEE Trans. Commun.*, vol. 48, pp. 679–691, Apr. 2000.

[4] M. Z. Win and R. A. Scholtz, "On the robustness of ultra -wide bandwidth signals in dense multipath environments," *IEEE Commun. Lett.*, vol. 2, pp. 51–53, Feb. 1998.

[5] M. Z. Win, "A unified spectral analysis of generalized time-hopping spread-spectrum signals in the presence of timing jitter," *IEEE J. Select. Areas Commun.*, vol. 20, pp. 1664-1676, Dec. 2002.

[6] A. Ridolfi and M. Z. Win, "Ultrawide bandwidth signals as shot-noise: a unifying approach," *IEEE J. Select. Areas Commun.*, vol. 24, no. 4, pp. 899-905, Apr. 2006.

[7] S. S. Kolenchery, J. K. Townsend, and J. A. Freebersyser, "A novel impulse radio network for tactical military wireless communications," in *Proc. Military Comm. Conf.*, vol. 1, pp. 59–65, Oct. 1998, Boston, MA.

[8] J. Conroy, J. L. LoCicero, and D. R. Ucci, "Communication techniques using monopulse waveforms," in *Proc. Military Comm. Conf.*, vol. 2, pp. 1181–1185, Oct. 1999.

[9] J. R. Foerster, "The effects of multipath interference on the performance of UWB systems in an indoor wireless channel," in *Proc. IEEE Semiannual Veh. Technol. Conf.*, vol. 2, pp. 1176–1180, May 2001, Rhodos, GREECE.

[10] L. Zhao and A. M. Haimovich, "Interference suppression in ultra-wideband communications," in *Proc. Conf. on Inform. Sci. and Sys.*, vol. 2, pp. 759–763, Mar. 2001.

[11] M. L. Welborn, "System considerations for ultra-wideband wireless networks," in *Proc. IEEE Radio and Wireless Conf.*, pp. 5–8, Aug. 2001, Boston, MA.

[12] L. Yang and G. B. Giannakis, "Impulse radio multiple access through ISI channels with multi-stage block-spreading," in *Proc. of IEEE Conference on Ultra Wideband Systems and Technologies*, 2002.

[13] E. Fishler and H. V. Poor, "On the tradeoff between two types of processing gains," *IEEE Trans. Commun.*, vol. 53, pp. 1744–1753, Oct. 2005.

[14] R. C. Qiu, "A study of the ultra-wideband wireless propagation channel and optimum UWB receiver design," *IEEE J. Select. Areas Commun.*, vol. 20, pp. 1628–1637, Feb. 1999.

[15] R. C. Qiu *et al.*, "Ultra-wideband for multiple-access communications," *IEEE Commun. Mag.*, vol. 43, pp. 80–87, Feb. 2005.

[16] "New Public Safety Applications and Broadband Internet Access among Uses Envisioned by FCC Authorization of Ultra-Wideband Technology," in *FCC News Report*, Feb. 2002, (et docket no. 98-153).

[17] M. Z. Win and R. A. Scholtz, "Comparisons of analog and digital impulse radio for multiple -access communications," in *Proc. IEEE Int. Conf. on Commun.*, vol. 1, pp. 91–95, June 1997, Montréal, CANADA.

[18] M. Z. Win *et al.*, "ATM-based TH-SSMA network for multimedia PCS," *IEEE J. Select. Areas Commun.*, vol. 17, pp. 824–836, May 1999.

[19] A. F. Molisch *et al.*, "A low-cost time-hopping impulse radio system for high data rate transmission," *Eurasip J. Applied Signal Processing, special issue on UWB*, vol. 35, 2005, (invited).

[20] A. F. Molisch *et al.*, "UWB PHY proposal for IEEE 802.15.4a Alt-PHY Project," *IEEE document 802.15-05-0172-02-004a*, Mar. 2005.

[21] P. Runkle *et al.*, "DS-CDMA: the modulation technology of choice for UWB communications," in *IEEE Conference on Ultra Wideband Systems and Technologies*, pp. 364 – 368, Nov. 2003.

[22] A. Batra, "Multi-band OFDM physical layer proposal," in *Document IEEE 802.15-03/267r2*, 2003.

[23] A. F. Molisch, *Wireless Communications*. IEEE-Press Wiley, 2005.

[24] M. Z. Win and Z. A. Kostić, "Virtual path analysis of selective Rake receiver in dense multipath channels," *IEEE Commun. Lett.*, vol. 3, pp. 308–310, Nov. 1999.

[25] M. Z. Win, G. Chrisikos, and N. R. Sollenberger, "Performance of Rake reception in dense multipath channels: implications of spreding bandwidth and selection diversity order," *IEEE J. Select. Areas Commun.*, vol. 18, pp. 1516–1525, Aug. 2000.

[26] M. Z. Win and G. Chrisikos, *Wideband Wireless Digital Communications*, ch. Impact of spreading bandwidth and selection diversity order on selective Rake reception. U.K.: Prentice-Hall, 2001, A. F. Molisch(ed.).
[27] J. D. Choi and W. E. Stark, "Performance of ultra-wideband communications with suboptimal receivers in multipath channels," *IEEE J. Select. Areas Commun.*, vol. 20, pp. 1754–1766, Dec. 2002.
[28] M. Z. Win and R. A. Scholtz, "On the energy capture of ultra-wide bandwidth signals in dense multipath environments," *IEEE Commun. Lett.*, vol. 2, pp. 245–247, Sept. 1998.
[29] M. Z. Win, R. A. Scholtz, and M. A. Barnes, "Ultra-wide bandwidth signal propagation for indoor wireless communications," in *Proc. IEEE Int. Conf. Commun.*, vol. 1, pp. 56–60, June 1997, Montréal, CANADA.
[30] M. Z. Win and R. A. Scholtz, "Characterization of ultra-wide bandwidth wireless indoor channels: A communication-theoretic view," *IEEE J. Select. Areas Commun.*, vol. 20, pp. 1613–1627, Dec. 2002.
[31] D. Cassioli, M. Z. Win, and A. F. Molisch, "The UWB indoor channel: from statistical model to simulations," *IEEE J. Select. Areas Commun.*, vol. 20, pp. 1247–1257, Aug. 2002.
[32] A. F. Molisch, J. R. Foerster, and M. Pendergrass, "Channel models for ultrawideband personal area networks," *IEEE Pers. Commun. Mag.*, vol. 10, pp. 14–21, Dec. 2003.
[33] A. F. Molisch, "Ultrawideband propagation channels - theory, measurement, and modeling," *IEEE Trans. on Veh. Technol.*, vol. 54, pp. 1528–1545, Sept. 2005.
[34] J. Karedal *et al.*, "UWB channel measurements in an industrial environment," in *Proc. IEEE Global Telecomm. Conf.*, pp. 3511–3516, 2004.
[35] R. Maffei, U. Manzoli, and M. L. Merani, "Rake reception with unequal power path signals," *IEEE Trans. Commun.*, vol. 52, pp. 24–27, Jan. 2004.
[36] D. Cassioli *et al.*, "Performance of low-complexity Rake reception in a realistic UWB channel," in *Proc. IEEE Int. Conf. on Commun.*, vol. 2, pp. 763–767, May 2002.
[37] W. Suwansantisuk, M. Z. Win, and L. A. Shepp, "On the performance of wide-bandwidth signal acquisition in dense multipath channels," *IEEE Trans. Veh. Technol.*, vol. 54, no. 5, pp. 1584-1594, Sept. 2005.
[38] W. Suwansantisuk and M. Z.Win, "Multipath aided rapid acquisition: Optimal search strategies," *IEEE Trans. Inform. Theory*, vol. 52, Jan. 2007.
[39] L. M. Jalloul and J. M. Holtzman, "Multipath fading effect on wideband DS/CDMA signals: Analysis, simulation, and measurements," *IEEE Trans. on Veh. Technol.*, vol. 43, pp. 801–807, Aug. 1994.
[40] D. L. Noneaker and M. B. Pursley, "On the chip rate of CDMA systems with doubly selective fading reception," *IEEE J. Select. Areas Commun.*, vol. 12, pp. 853–861, June 1994.
[41] D. Goeckel and W. Stark, "Performance of coded direct-sequence systems with Rake reception in a multipath fading environment," *European Trans. on Telecommun., Special Issue on Spread Spectrum Techniques*, vol. 6, pp. 41–52, Jan.-Feb. 1995.
[42] T. Eng and L. B. Milstein, "Coherent DS-CDMA performance in Nakagami multipath fading," *IEEE Trans. Commun.*, vol. 43, pp. 1134–1143, Feb./Mar./Apr. 1995.
[43] J. G. Proakis, ed., *Digital Communications*. New York, NY, 10020:: McGraw-Hill, Inc., 4th Ed., 2001.
[44] J. R. Foerster, "Channel modeling sub-committee report final," in *Tech. Rep. P802.15 02/490r1, IEEE 802.15 SG3a*, Feb. 2003.
[45] A. F. Molisch *et al.*, "IEEE 802.15.4a channel model - final report," Nov. 2004.
[46] A. A. Saleh and R. A. Valenzuela, "A statistical model for indoor multipath propagation," *IEEE J. Select. Areas Commun.*, vol. 5, pp. 128–137, Feb. 1987.
[47] S. S. Ghassemzadeh *et al.*, "UWB indoor path-loss model for residential and commercial buildings," in *Proc. IEEE Semiannual Veh. Technol. Conf.*, vol. 5, pp. 3115 – 3119, Oct. 2003, Fall.
[48] W. C. Lau, M.-S. Alouini, and M. K. Simon, "Optimum spreading bandwidth for selective Rake reception over Rayleigh fading channels," *IEEE J. Select. Areas Commun.*, vol. 19, pp. 1080–1089, June 2001.
[49] M. Z. Win *et al.*, "On the SNR penalty of MPSK with hybrid selection/maximal ratio combining over i.i.d. Rayleigh fading channels," *IEEE Trans. Commun.*, vol. 51, pp. 1012–1023, June 2003.
[50] M. Z. Win and Y. Wen, "Extreme power dispersion profiles for Nakagami-m fading channels with maximal-ratio diversity," *IEEE Commun. Lett.*, vol. 9, no. 5, pp. 385-387, May 2005.
[51] M. Z. Win, "On the monotonicity of matched-filter bounds for diversity combining receivers," in *Proc. IEEE Global Telecomm. Conf.*, vol. 3, San Francisco, CA, Dec. 2003, pp. 1684-1688.

Dajana Cassioli (S'02, M'04)received the "Laurea" degree and the Ph.D. degree from the University of Rome Tor Vergata, Italy, in 1999 and in 2003, respectively. From 1998 to 1999, she has been with the Fondazione Ugo Bordoni, Rome, Italy, where she was involved in the study of semiconductor optical amplifiers and in the development of computer models of devices for WDM optical communication systems. In 1999, she joined the Communication Group of the Electronic Engineering Department of the University of Rome Tor Vergata, where she has been working on the analysis and simulation of the TD-CDMA Radio Interface of the UMTS system. She is currently with RADIOLABS, a university-industry research consortium for the development of radio technologies, where she is the Director of the Associate Laboratory of RADIOLABS at the University of L'Aquila, Italy. She has been the scientific officer responsible in RADIOLABS for the IST project ULTRAWAVES, Contract n. IST-2001-35189, funded by the European Community within the Fifth Framework. In ULTRAWAVES she contributed to the characterization of the UWB propagation channel and to the measurements and modeling of the UWB interference over UMTS, WLANs IEEE 802.11 and Bluetooth. She is currently involved in the IST Integrated Project PULSERS, funded by the European Community within the Sixth Framework. Her main research interests are in the field of wireless access technologies, and in particular the UWB radio technology, ad-hoc networks and Bluetooth. In the year 2000, she was a Summer Manager with the Wireless Systems Research Department at AT&T Labs-Research, working on the statistical analysis of UWB signal propagation.

Moe Z. Win (S'85-M'87-SM'97-F'04) received the B.S. degree (*magna cum laude*) from Texas A&M University, College Station, in 1987 and the M.S. degree from the University of Southern California (USC), Los Angeles, in 1989, both in Electrical Engineering. As a Presidential Fellow at USC, he received both an M.S. degree in Applied Mathematics and the Ph.D. degree in Electrical Engineering in 1998.

Dr. Win is an Associate Professor at the Massachusetts Institute of Technology (MIT). Prior to joining MIT, he spent five years at AT&T Research Laboratories and seven years at the Jet Propulsion Laboratory. His main research interests are the applications of mathematical and statistical theories to communication, detection, and estimation problems. Specific current research topics include measurement and modeling of time-varying channels, design and analysis of multiple antenna systems, ultra-wide bandwidth (UWB) systems, optical transmission systems, and space communications systems.

Professor Win has been actively involved in organizing and chairing a number of international conferences. He served as the Technical Program Chair for the IEEE Conference on Ultra Wideband in 2006, the IEEE Communication Theory Symposia of ICC-2004 and Globecom-2000, and the IEEE Conference on Ultra Wideband Systems and Technologies in 2002; Technical Program Vice-Chair for the IEEE International Conference on Communications in 2002; and the Tutorial Chair for the IEEE Semiannual International Vehicular Technology Conference in Fall 2001. He served as a chair (2004-2006) and secretary (2002-2004) for the Radio Communications Committee of the IEEE Communications Society. Dr. Win is currently an Editor for *IEEE Transactions on Wireless Communications.* He served as Area Editor for *Modulation and Signal Design* (2003-2006), Editor for *Wideband Wireless and Diversity* (2003-2006), and Editor for *Equalization and Diversity* (1998-2003), all for the *IEEE Transactions on Communications*. He was Guest-Editor for the 2002 *IEEE Journal on Selected Areas in Communications* (Special Issue on Ultra-Wideband Radio in Multiaccess Wireless Communications).

Professor Win received the International Telecommunications Innovation Award from Korea Electronics Technology Institute in 2002, a Young Investigator Award from the Office of Naval Research in 2003, and the IEEE Antennas and Propagation Society Sergei A. Schelkunoff Transactions Prize Paper Award in 2003. In 2004, Dr. Win was named Young Aerospace Engineer of the Year by AIAA, and garnered the Fulbright Foundation Senior Scholar Lecturing and Research Fellowship, the Institute of Advanced Study Natural Sciences and Technology Fellowship, the Outstanding International Collaboration Award from the Industrial Technology Research Institute of Taiwan, and the Presidential Early Career Award for Scientists and Engineers from the United States White House. He was honored with the 2006 IEEE Eric E. Sumner Award "for pioneering contributions to ultra-wide band communications science and technology." Professor Win is an IEEE Distinguished

Lecturer and elected Fellow of the IEEE, cited "for contributions to wideband wireless transmission."

Francesco Vatalaro received the Dr. Ing. degree in Electronics Engineering from the University of Bologna, Italy. He was with Fondazione Ugo Bordoni, FACE Standard, and Selenia Spazio, Italy. In 1987, he became an Associate Professor of Radio Systems at the University of Roma Tor Vergata, Italy, where he is presently Full Professor. In 2000 he was Visiting Professor at the University of California Los Angeles, CA. Since 1985 he collaborates in and coordinates several telecommunications projects within national Italian and European programmes. He was a co-winner of the 1990 "Piero Fanti" INTELSAT/Telespazio international prize. He is the President of RADIOLABS, a university-industry research consortium for the development of radio technologies. He is the Principal Investigator of the Italian national project VICOM (Virtual Immersive Communications) with budget of 12500 keuro (2002-2006). He is a member of the Editorial Board of the *Int. J. of Satellite Communications* (J. Wiley). He is the Chairman of the IEEE joint Vehicular Technology/Communications Society Italy Chapter, and is/was a member of several Scientific Committees. He is the author of more than 150 scientific papers.

Andreas F. Molisch (S'89, M'95, SM'00, F'05) received the Dipl. Ing., Dr. techn., and habilitation degrees from the Technical University Vienna (Austria) in 1990, 1994, and 1999, respectively. From 1991 to 2000, he was with the TU Vienna, becoming an associate professor there in 1999. From 2000-2002, he was with the Wireless Systems Research Department at AT&T (Bell) Laboratories Research in Middletown, NJ. Since then, he has been with Mitsubishi Electric Research Labs, Cambridge, MA, USA, where he is now a Distinguished Member of Technical Staff. He is also professor and chairholder for radio systems at Lund University, Sweden.

Dr. Molisch has done research in the areas of SAW filters, radiative transfer in atomic vapors, atomic line filters, smart antennas, and wideband systems. His current research interests are MIMO systems, measurement and modeling of mobile radio channels, and UWB. Dr. Molisch has authored, co-authored or edited four books, among them the recent textbook *Wireless Communications* (Wiley-IEEE Press), eleven book chapters, some 95 journal papers, and numerous conference contributions.

Dr. Molisch is an editor of the *IEEE Transactions on Wireless Communications*, co-editor of a recent special issue on MIMO and smart antennas in *J. Wireless Comm. Mob. Comp.*, and co-editor of an upcoming *IEEE JSAC* special issue on UWB. He has been member of numerous TPCs, vice chair of the TPC of VTC 2005 spring, and will be general chair of ICUWB 2006. He has participated in the European research initiatives "COST 231," "COST 259," and "COST273," where he was chairman of the MIMO channel working group, and is also chairman of Commission C (signals and systems) of URSI (International Union of Radio Scientists). Dr. Molisch is a Fellow of the IEEE and recipient of several awards.